Histol Histopathol (2024) 39: 659-670

Histology and Histopathology
From Cell Biology to Tissue Engineering

ORIGINAL ARTICLE Open Access

The promoting effects of Grin2d expression in tumorigenesis and the aggressiveness of esophageal cancer

Ling-ling Wang[1], Jun Li[2], Hang Xue[3], Li Zhang[3], Da-yong Yu[4], Ning Yang[3], Wen-jing Yun[3], Ming-zhen Zhao[5] and Hua-chuan Zheng[3]

[1]Department of Laboratory Medicine, The Affiliated Hospital of Chengde Medical University, Chengde, [2]Department of Thoracic Surgery, Shandong Provincial Hospital, Jinan, [3]Department of Oncology, The Affiliated Hospital of Chengde Medical University, [4]Department of Cell Biology, Basic Medicine College of Chengde Medical University and [5]Office of Research Affairs, The Affiliated Hospital of Chengde Medical University, Chengde, China

Summary. Grin2d is an ionotropic NMDA receptor, a subunit of glutamate-dependent, and a facilitator of cellular calcium influx in neuronal tissue. In this study, we found that Grin2d expression was higher in esophageal cancer than in normal mucosa at both the mRNA and protein level using RT-PCR, bioinformatics analysis, and western blotting ($p<0.05$). Grin2d mRNA expression was positively correlated with old age, white race, heavy weight, distal location, adenocarcinoma, cancer with Barrett's lesion, or high-grade columnar dysplasia ($p<0.05$). The differential genes associated with Grin2d mRNA were involved in fat digestion and absorption, cholesterol metabolism, lipid transfer, lipoproteins, synaptic membranes, and ABC transporters ($p<0.05$). The Grin2d-related genes were classified into the following categories: metabolism of glycerolipids, galactose, and O-glycan, cell adhesion binding, actin binding, cadherin binding, the Hippo signaling pathway, cell-cell junctions, desmosomes, DNA-transcription activator binding, and skin development and differentiation ($p<0.05$). Grin2d immunoreactivity was positively correlated with distal metastasis and unfavorable overall survival in esophageal cancer ($p<0.05$). Grin2d overexpression promoted proliferation, migration, and invasion in esophageal cancer cells but blocked apoptosis ($p<0.05$) and increased the expression of PI3K, Akt and p-mTOR. Grin2d knockout caused the opposite effects. These findings indicated that upregulated Grin2d expression played an important role in esophageal carcinogenesis via the PI3K/Akt/mTOR pathway and might be a biological marker for aggressive tumor behavior and poor prognosis. Its silencing might represent a targeted therapy approach against esophageal cancer.

Key words: Esophageal cancer, Grin2d, Biological behaviors, Prognosis, Gene therapy

Corresponding Author: Hua-chuan Zheng, Department of Oncology, The Affiliated Hospital of Chengde Medical University, Chengde, PR China. e-mail: zheng_huachuan@hotmail.com

www.hh.um.es. DOI: 10.14670/HH-18-674

Introduction

The glutamate (Glu) system is a very complicated bioregulatory pathway composed of several ionotropic Glu receptors (iGlu.Rs), Glu transporters (EAATs), metabotropic Glu receptors (mGlu.Rs), and glutamine synthetase (GS) to metabolize glutamate into glutamine. N-methyl-D-aspartate receptors (NMDAR) are ionotropic glutamate receptors that include the kainate and AMPA receptors and serve as heterotetrameric, ligand-gated ion channels with high calcium permeability and voltage-dependent sensitivity to magnesium. The binding of the neurotransmitter Glu to the epsilon subunit and glycine to the zeta subunit coupled with membrane depolarization to eliminate channel inhibition by Mg^{2+} can activate these channels. The channels are heteromers consisting of the core receptor subunit NMDAR1 (GRIN1 or NR1) and one or more of the NMDAR2 (GRIN2 or NR2 or GluN2) A-D, or NR3 (A-B) subunits. NMDAR are cationic channels mainly permeable to Ca^{2+} (Camp and Yuan, 2020; Pałasz and Krzystanek, 2022). Hajdú et al. (2018) demonstrated that the NR1 and NR3 subunits can bind glycine, whereas the NR2 subunits bound glutamate to achieve full activation. NR1 may be involved in recognizing the nuclear localization signal (NLS) of importin-α.

NMDARs are essential for learning, memory, and

neuron development. Genetic variants of the *Grin2d* gene cause early-onset neurological disorders, particularly developmental and epileptic encephalopathy (DEE) and non-specific early-onset epileptic encephalopathy (Wollmuth et al., 2021). Andrews et al. (2020) reported that GluN2D$^{-/-}$ mice had an increase in PC and a decrease in DG, indicating reduced free fatty acids caused by brain ischemia. They also found that the GluN2D$^{-/-}$ mice had higher neurorecovery and neuroprotection rates from ischemic strokes than the wild-type mice. Sharma et al. identified novel, recurrent regulatory mutations affecting known cancer genes, such as NKX2-1 and Grin2d, in multiple cancer types. Zarei et al. (2021) found that specific dysregulated genes, including Grin2d, were involved in adult T-cell Leukemia/Lymphoma. Ma et al. (2021) found that Grin2d was a key exosomal hub mRNA for colorectal cancer.

The incidence of esophageal cancer (EC) has been increasing with changes in the environment and diet. The main types of EC are adenocarcinoma and squamous cell carcinoma, which develop in diverse locations in the esophagus and are driven by different genetic mutations. Squamous cell carcinoma is the most common type of EC. Its risk factors include older age, male gender, smoking, alcohol use, polycyclic aromatic hydrocarbons (PAHs), gastroesophageal reflux disease (GERD), dysplasia, and tooth loss. Nonsteroidal anti-inflammatory drugs, vitamins, vegetables, green tea, and fruit intake can prevent esophageal carcinogenesis. Management of EC depends on patient fitness and tumor stage. Endoscopic removal is used for early-stage tumors, while chemotherapy, chemo-radiotherapy, surgical resection, or a combination of these approaches are used for advanced tumors (Musa et al., 2021; Mwachiro et al., 2021; Zhao et al., 2021). Despite improvements in the management and treatment of EC, the general outcome remains very poor. Therefore, it is crucial to identify biomarkers and molecular targets.

Materials and methods

Cell culture and transfection

Esophageal squamous cancer cells (KYSE-150) were obtained from the Cell Bank of the Chinese Academy of Sciences, Shanghai, China. The cells were cultured in RPMI 1640 medium containing 10% fetal bovine serum (FBS), 100 units/mL penicillin, and 100 μg/mL streptomycin, in a humid environment of 5% CO_2 at 37°C. Plasmid pcDNA3.1-Grin2d-3×Flag was used to ectopically overexpress Grin2d, and pGPU6/GFP-shGrin2d was used to knockdown Grin2d. shGrin2d targeted the sequence 5'- AGGGTTTCTGCA TCGACATTC -3'. The KYSE-150 cells with a density of 2.0×10^5 per well were seeded in a 6-well plate to reach 60-80% confluency before transfection. After replacing RPMI 1640 medium lacking serum and antibiotic, the cells were treated with a plasmid DNA-lipid complex composed of 250 μl serum-free medium Opti-MEM, 2.5μg plasmid DNA, 5μl P3000^{TM} Rergent (Invitrogen, USA), and 7.5 μl lipofectamine 3000^{TM} Rergent (Invitrogen, USA). Cells were incubated for 48h at 37°C in a humid environment of 5% CO_2. Then, transfected cells were analyzed.

Proliferation assay

The number of viable cells was determined using Cell Counting Kit-8 (CCK-8, ReportBio, China). Briefly, 2.0×10^3 cells/well were seeded in a 96-well plate. At different time points, the CCK-8 solution (10 μL) was added to each well. The plates were incubated for 3h in a humid environment of 5% CO_2 at 37°C, and then measured at 450 nm using a micro-plate reader (Multiskan FC microplate photometer, USA).

Apoptosis assay

Flow cytometry with 7-amino-actinomycin (7-AAD) and phycoerythrin (PE)-labeled annexin V (BD Pharmingen, USA) was used to detect phosphatidyl-serine externalization, an indicator of early apoptosis (REF). KYSE-150 cells were collected by trypsinization, washed with 1×PBS, and centrifuged to harvest the cells. The cells were resuspended in 1×Binding Buffer at a density of 8.0×10^5 cells/ml. 100 μl of the binding buffer, 5 μl of PE-labeled annexin V and 5 μl of 7-AAD were incubated in a 5 ml culture tube for 15 min at 25°C in the dark. Then, cells were analyzed by flow cytometer (Navios, USA).

Wound healing assay

KYSE-150 cells (1.0×10^6 cells/well) were seeded in 6-well culture plates. When the cells reached 80-90% confluence, the monolayer was scratched with a 200 μl pipette tip, washed three times with 1×PBS, and cultured in FBS-free medium. After 24h, the cells were photographed, and the scratch area was measured using Image J software (v1.8.0, National Institutes of Health, USA).

Cell migration and invasion assays

For the migration assay, KYSE-150 cells (2.5×10^5) were resuspended in serum-free RPMI 1640 and seeded in the control-membrane insert in the top portion of the transwell chamber (BD Bioscience, USA). The lower compartment of the chamber was filled with medium containing 10% FBS as a chemo-attractant. For the invasion assay, the membranes were coated with Matrigel (BD Bioscience, USA) and incubated for 4h at 37°C. The procedures were the same as for the migration assay, excluding the Matrigel-coated insert. After incubating at 37°C for 24h, the cells on the membrane were scrubbed, washed three times with 1×PBS, fixed in 100% methanol for 20 min, and stained with Giemsa dye for 5 min. The number of migrated and invaded KYSE-

150 cells was counted under an inverted microscope.

Patients

Paraffin-embedded esophageal cancer tumors (n=333), paraffin-embedded normal mucosa (n=148), frozen esophageal cancer tumors and matched normal mucosa (n=17) were collected to construct a tissue microarray and for protein extraction from The First Affiliated Hospital of Jinzhou Medical University (China) between 2020.1 and 2021.12. Tissue (297 cases of esophageal cancer tumors and 238 cases of normal mucosa) and cDNA microarrays (67 cases of esophageal cancer tumors and 28 cases of normal mucosa) were purchased from Shanghai Outdo Biotech (Shanghai) and used for immunohistochemistry and RT-PCR, respectively. None of the patients received preoperative chemotherapy, radiotherapy, or adjuvant therapy. All the patients provided written consent to use tumor tissue for clinical studies, and the Ethics Committee of the Affiliated Hospital of Chengde Medical University approved the study protocol (NO. CYFYLL2020230). All methods were performed in accordance with the relevant guidelines and regulations. We had no access to information that could identify individual participants during or after data collection.

RT-PCR

The real-time PCR primers were designed using primer-BLAST in NCBI based on the GenBank sequences. The primer sequences were forward 5'-GTCTCCTCTGACTTCAACAGCG-3' and reverse 5'-ACCACCCTGTTGCTGTAGCCAA-3' for GAPDH (131 bp); forward 5'-CCTCAGTCCTGTTGGTTAC-3' and reverse 5'-GAAGATGACGGCGAAGAA-3', for Grin2d (190 bp). Real-time PCR was carried out with iTaqTM Universal SYBR® Green Supermix (BIO-RAD, USA, 172-5121) using the CFX96™ real-time system (BIO-RAD, Bio-Rad Laboratories, Inc., Singapore). GAPDH was used as an internal control. After the cDNA microarray plates were transiently centrifuged, 10 µl qPCR mix (2×) with 1 µl (10 µM) of each primer, and 7 µl of RNase-free ddH2O were added to them. The protocol was predenaturation at 95°C for 15 min, followed by 45 cycles of denaturation at 95°C for 10 s, annealing at 60°C for 20 s, and then extension at 72°C for 30 s.

Western blotting

Total proteins were obtained from fresh tissue samples and cells using RIPA lysis buffer and quantified with the BCA Protein Assay kit (NCM, Suzhou, China, WB6502). Proteins of equal amounts were separated by 10% SDS-PAGE and then transferred to PVDF membranes. Non-specific antigen sites were blocked with 5% skim milk for 1.5h at room temperature and then incubated with rabbit anti-Grin2d (1:500, Alomone Labs, AGC-020), mouse anti-Ki-67 (1:1000, Proteintech, 39799), rabbit anti-p27 (1:500, Wanleibio,WL04174), rabbit anti-PI3K (1:1000, CST, 4249s), rabbit anti-Slug (1:1000, Abcam, ab302780), rabbit anti-Akt (1:1000, Proteintech 10176-2-AP), mouse anti-p-mTOR (1:2000, Proteintech, 67778-1-Ig), mouse anti-PARP-1 (1:500, Santa Cruz, sc-8007), rabbit anti-XIAP (1:500, Immunoway, YT4913), goat anti-p-CDC-25c (1:500, Santa Cruz, sc-327), mouse anti-MMP9 (1:500, Santa Cruz, sc-393859), or mouse anti-GAPDH (1:2000, Proteintech, 60004-1-Ig) overnight at 4°C. The membranes were washed three times with 1×TBST and then incubated with an anti-rabbit (1:5000, CST, USA, #7074S), anti-mouse (1:5000, CST, USA, #7076S), or anti-goat (1:5000, Abcam, UK, #ab205723S) secondary antibody with horseradish peroxidase for 2h at room temperature. Protein bands were captured with the C300 (Azure Biosystems, Inc, USA) using the WesternBright™ ECL Kit (Advansta, USA, K-12045-D50), and densitometry was performed using ImageJ software (v1.8.0, National Institutes of Health, USA).

Tissue microarray (TMA)

Tissue samples (esophageal cancer tumors and normal mucosa) were fixed with 4% paraformaldehyde, dehydrated in alcohol, dealcoholized in xylene, and embedded in paraffin. For histological analysis, 4-µm-thick sections were prepared from the paraffin blocks and stained with hematoxylin and eosin. Representative regions of the adjacent normal tissue and solid tumors were observed by microscopy, and corresponding tissue cores were removed from the paraffin blocks to generate the TMA.

Immunohistochemistry (IHC)

After baking at 60°C for 2h, the sections were dewaxed in xylene and rehydrated in graded alcohol three times. Antigen repair was performed by microwaving the samples in 0.01M sodium citrate buffer (pH=6) for 20 min. Endogenous peroxidase activity and non-specific binding were blocked with 3% hydrogen peroxide (H_2O_2) and 5% bovine serum albumin (BSA), respectively, for 30 min each. The sections were incubated with rabbit anti-Grin2d antibody (1:500, Alomone Labs, Israel, AGC-020) for 3h at room temperature. The sections were washed three times with 1×PBS and then incubated with polyclonal swine anti-rabbit antibody with horseradish peroxidase (1:200, DAKO, Japan, P0399) at room temperature for 2h. The sections were washed three times with 1×PBS and then the staining was visualized with diaminobenzidine (DAB). After staining with hematoxylin, the sections were dehydrated, dried, sealed, and visualized by microscopy (Nikon, Nikon Corporation, Japan). The evaluation of the IHC staining was previously described (Yu et al., 2007).

Bioinformatics analysis

The expression of the Grin2d gene was analyzed using the xiantao platform (https://www.xiantao.love/) and the UALCAN database (http://ualcan.path.uab.edu/). Grin2d mRNA expression data (RNA-seqV2) and esophageal cancer clinicopathological data were extracted using R software (v3.6.3) from TCGA database (https://portal.gdc.cancer.gov/). The prognostic significance of Grin2d was explored using the Kaplan-Meier plotter (https://kmplot.com/analysis/). In addition, we screened the differential genes with xiantao platform. The differential genes were used to construct a PPI network and select important hub genes using STRING (https://cn.string-db.org/) and Cytoscape (v3.7.0). These genes were subjected to GO + KEGG and GSEA analysis with the xiantao platform to identify signaling pathways.

Statistical analysis

SPSS 23.0 was used to conduct the chi-square test and cox analysis. Spearman correlation analysis, student t-test, and log-rank test were employed to compare the different rates, differences between two groups, and survival analysis, respectively. Cox's hazard proportional regression was used to perform multivariate survival analysis. $p<0.05$ was considered statistically significant.

Results

The clinicopathological and prognostic significances of Grin2d mRNA expression in esophageal cancer

We found a higher Grin2d mRNA expression in esophageal cancer than in normal mucosa of the

Table 1. The relationship between Grin2d mRNA expression and the clinicopathological characteristics of esophageal cancer.

Characteristic	Variable	Low expression	High expression	p
Age, median (IQR)		57 (51, 69)	62 (57, 74)	0.012
Gender, n (%)	Female	13 (8%)	10 (6.2%)	0.653
	Male	68 (42%)	71 (43.8%)	
Race, n (%)	Asian	27 (18.8%)	11 (7.6%)	0.007
	Black or Afr-Ame	4 (2.8%)	2 (1.4%)	
	White	43 (29.9%)	57 (39.6%)	
Weight, n (%)	≦70	48 (30%)	28 (17.5%)	0.003
	>70	32 (20%)	52 (32.5%)	
BMI, n (%)	≦25	49 (32%)	35 (22.9%)	0.043
	>25	28 (18.3%)	41 (26.8%)	
Tumor central location, n (%)	Distal	49 (30.4%)	64 (39.8%)	0.022
	Mid	28 (17.4%)	14 (8.7%)	
	Proximal	4 (2.5%)	2 (1.2%)	
Barrett's esophagus, n (%)	No	57 (43.2%)	49 (37.1%)	0.025
	Yes	7 (5.3%)	19 (14.4%)	
T stage, n (%)	T1	11 (7.6%)	16 (11%)	0.173
	T2	19 (13.1%)	18 (12.4%)	
	T3	42 (29%)	35 (24.1%)	
	T4	4 (2.8%)	0 (0%)	
N stage, n (%)	N0	38 (26.4%)	28 (19.4%)	0.111
	N1	27 (18.8%)	36 (25%)	
	N2	7 (4.9%)	2 (1.4%)	
	N3	2 (1.4%)	4 (2.8%)	
M stage, n (%)	M0	67 (51.9%)	54 (41.9%)	0.468
	M1	3 (2.3%)	5 (3.9%)	
Pathologic stage, n (%)	Stage I	5 (3.5%)	11 (7.7%)	0.134
	Stage II	42 (29.6%)	27 (19%)	
	Stage III	25 (17.6%)	24 (16.9%)	
	Stage IV	3 (2.1%)	5 (3.5%)	
Histological type, n (%)	Ad	22 (13.6%)	58 (35.8%)	< 0.001
	Sq	59 (36.4%)	23 (14.2%)	
Histologic grade, n (%)	G1	9 (7.1%)	7 (5.6%)	0.213
	G2	38 (30.2%)	28 (22.2%)	
	G3	18 (14.3%)	26 (20.6%)	
Columnar mucosa dysplasia, n (%)	High grade	4 (5.9%)	21 (30.9%)	0.002
	Low grade	2 (2.9%)	3 (4.4%)	
	Negative	22 (32.4%)	16 (23.5%)	

esophagus by real-time RT-PCR, UALCAN and xiantao databases (Fig. 1A-C, $p<0.05$). Similarly, there was higher Grin2d expression in Caucasian cancer patients compared to Asian cancer patients, in 61-80-year-old patients than in 41-60 and 21-40-year-old cancer patients ($p<0.05$), in extremely obese patients than in extremely weight patients (extremely weight patients: $25\leq BMI<30$, $p<0.05$), and in G3 compared to G2 cancer patients based on the UALCAN database or real-time RT-PCR (Fig. 1D, $p<0.05$). We also observed higher Grin2d mRNA expression in M0 cancer patients than in M1 cancer patients (Fig. 1E, $p<0.05$) by real-time PCR. As shown in Table 1, Grin2d mRNA expression was positively correlated with old age, white race, heavy weight, distal location, cancer with Barrett's lesion, and high-grade columnar dysplasia ($p<0.05$). Adenocarcinoma had higher Grin2d expression than squamous cell carcinoma ($p<0.05$). Grin2d mRNA expression was negatively correlated with a long overall survival time for the adenocarcinoma patients ($p<0.05$), but the converse results were observed for adenocarcinoma and squamous cell carcinoma patients with a low mutational burden (Fig. 1F, $p<0.05$).

The Grin2d-related genes and signaling pathways in esophageal cancer

Using the xiantao platform, we found differentially expressed genes between the low and high Grin2d mRNA expression groups in esophageal cancer and built a volcano map (Fig. 2A). KEGG analysis showed that the top signaling pathways included fat digestion and absorption, cholesterol metabolism, lipid transfer, lipoproteins, synaptic membranes, and ABC transporters (Fig. 2B, $p<0.05$). Among the top differentially expressed genes, NANOS3, ABCG5, SOST, PAX1, NBAAT, and FOXI3 expression levels were higher in esophageal cancer than in normal tissue (Fig. 2C, $p<0.05$). Moreover, we obtained PPI pairs using STRING (Fig. 3A) and used Cytoscape to determine the top ten nodes ranked by degree (Fig. 3B). According to the xiantao database, the GALNT12 and MUC5AC expression levels were lower in esophageal cancer than in normal tissue (Fig. 3C, $p<0.05$), whereas MUCL1 expression levels were higher (Fig. 3C, $p<0.05$).

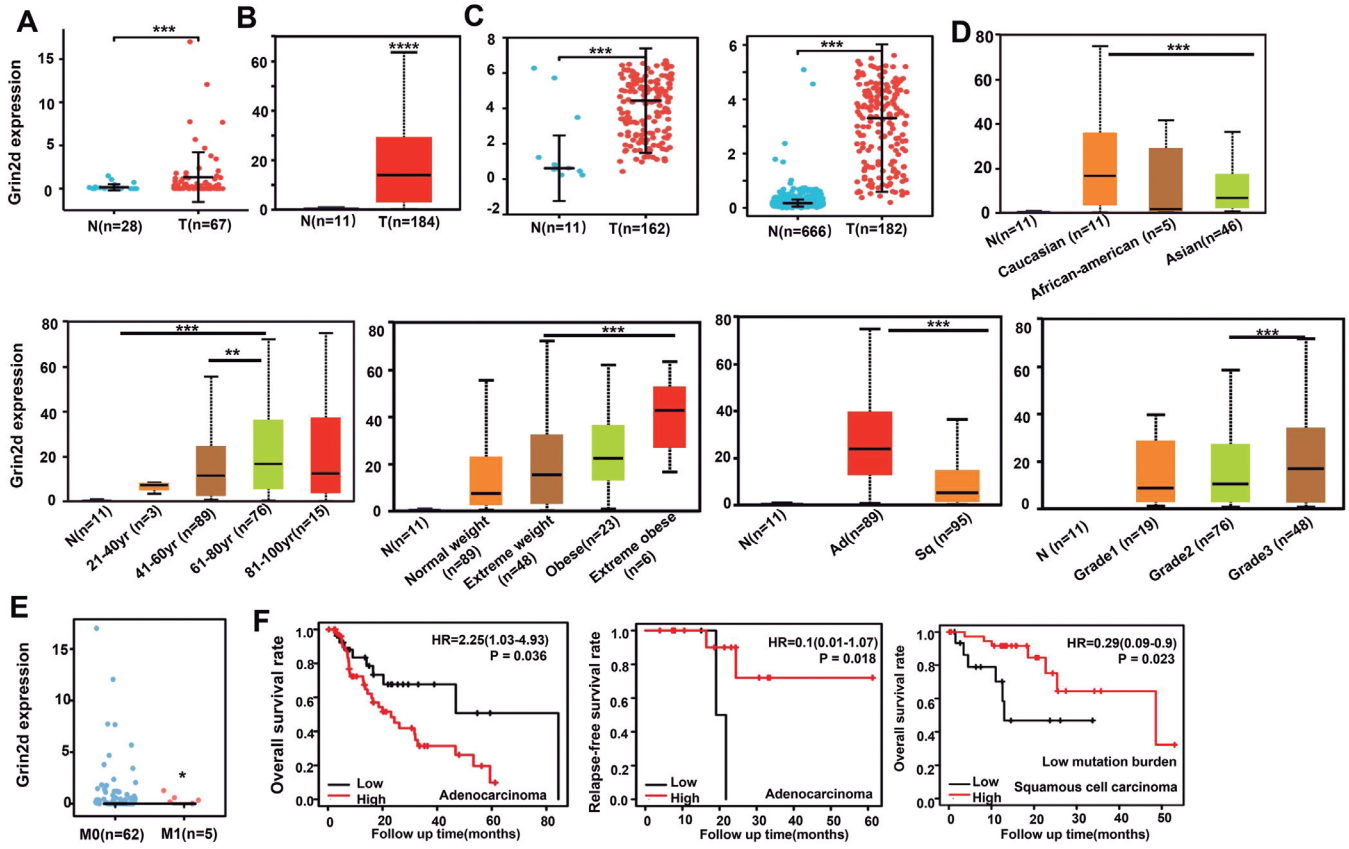

Fig. 1. The clinicopathological and prognostic significance of Grin2d mRNA expression according to bioinformatics analysis. Grin2d mRNA expression was higher in esophageal cancer than in normal mucosa according to real-time PCR **(A)** and the UALCAN **(B)** and xiantao databases (**C**, $p<0.05$). Grin2d mRNA expression was compared with the clinicopathological features of the esophageal cancer patients using the UALCAN database (**D**, $p<0.05$) and real-time PCR **(E)**. Its prognostic significance was analyzed using the Kaplan-Meier plotter **(F)**. N, normal; T, tumor; yr, years old; Ad, adenocarcinoma; Sq, squamous cell carcinoma; *, $p<0.05$; **, $p<0.01$; ***, $p<0.001$.

The genes positively correlated with Grin2d in esophageal cancer based on the xiantao database are shown in Figure 4A ($p<0.05$). These genes are involved in the metabolism of glycerolipids, galactose, and O-glycan, cell adhesion binding, actin binding, and cadherin binding (Fig. 4B). The genes negatively correlated with Grin2d in esophageal cancer are shown in Figure 4C ($p<0.05$). They are involved in the Hippo signaling pathway, cell-cell junctions, desmosomes, DNA-transcription activator binding, and skin development and differentiation (Fig. 4D). The Grin2d-correlated genes (FCHO1, AGMAT, PRAP1, FZD10, DLX5 and S1PR5) were expressed at higher levels in esophageal cancer compared to normal tissue (Fig. 4E, $p<0.05$).

The clinicopathological and prognostic significances of Grin2d protein expression in esophageal cancer

Based on the western blotting analysis, Grin2d protein levels were higher in esophageal cancer than in the matched normal tissue (Fig. 5A, $p<0.05$). Immunohistochemically, Grin2d protein was not

Table 2. Grin2d protein expression in normal tissue and esophageal cancer.

Groups		n	Grin2d expression				
			-	+	++	+++	PR (%)
Normal tissue vs primary cancer	Normal tissue	386	227	126	29	4	41.2
	Primary cancer	502	169	208	90	35	66.3
Primary cancer vs lymph node metastatic cancer	Primary cancer	502	169	208	90	35	66.3
	Lymph node metastatic cancer	128	53	51	18	6	58.6

PR, positive rate.

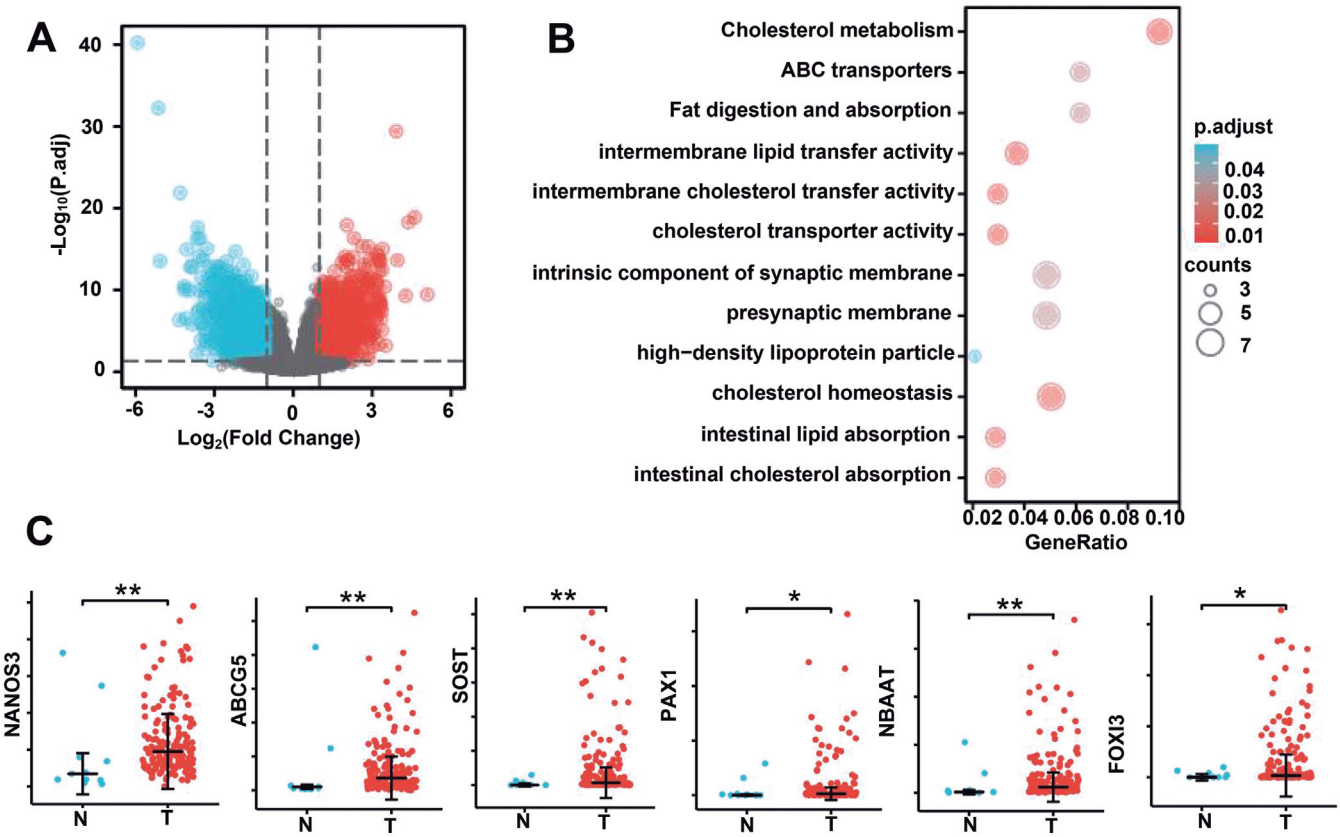

Fig. 2. The differential genes and related signaling pathways between low and high Grin2d expression in esophageal cancer. A volcano map of the differential genes between low and high Grin2d expression in esophageal cancer is shown **(A)**. These genes were subjected to signaling pathway analysis using KEGG **(B)**. The expression profiles and prognostic significance of these differential genes were studied using the xiantao platform **(C)**. N, normal; T, tumor; *, $p<0.05$; **, $p<0.01$.

Table 3. The relationship between Grin2d protein expression and the clinicopathological characteristics of esophageal cancer.

Clinicopathological features		n	Grin2d expression				
			-	+	++	+++	PR
Age (years)	<65	237	59	111	51	16	75.1
	≥65	201	68	71	36	26	66.2
Sex	Male	383	105	166	79	33	72.6
	Female	56	23	16	8	9	58.9
Depth of invasion	Tis-T2	84	23	37	19	5	72.6
	T3-T4	346	103	141	66	36	70.2
Venous invasion	-	366	103	157	73	33	71.9
	+	72	24	25	14	9	66.7
Lymph node metastasis	-	187	53	77	41	16	71.7
	+	242	73	99	44	26	69.8
Distant metastasis	-	425	125	179	83	38	70.6
	+	12	2	3	4	3	83.3
TNM staging	0-II	178	49	77	40	12	72.5
	III-IV	250	77	98	45	30	69.2
Differentiation	Well-differentiated	181	52	71	40	18	71.3
	Moderately-differentiated	204	60	90	36	18	70.6
	Poorly-differentiated	53	15	21	11	6	71.7
Tissue type	Squamous cell carcinoma	425	123	177	84	41	71.1
	Adenocarcinoma	14	5	5	3	1	64.3

PR, positive rate.

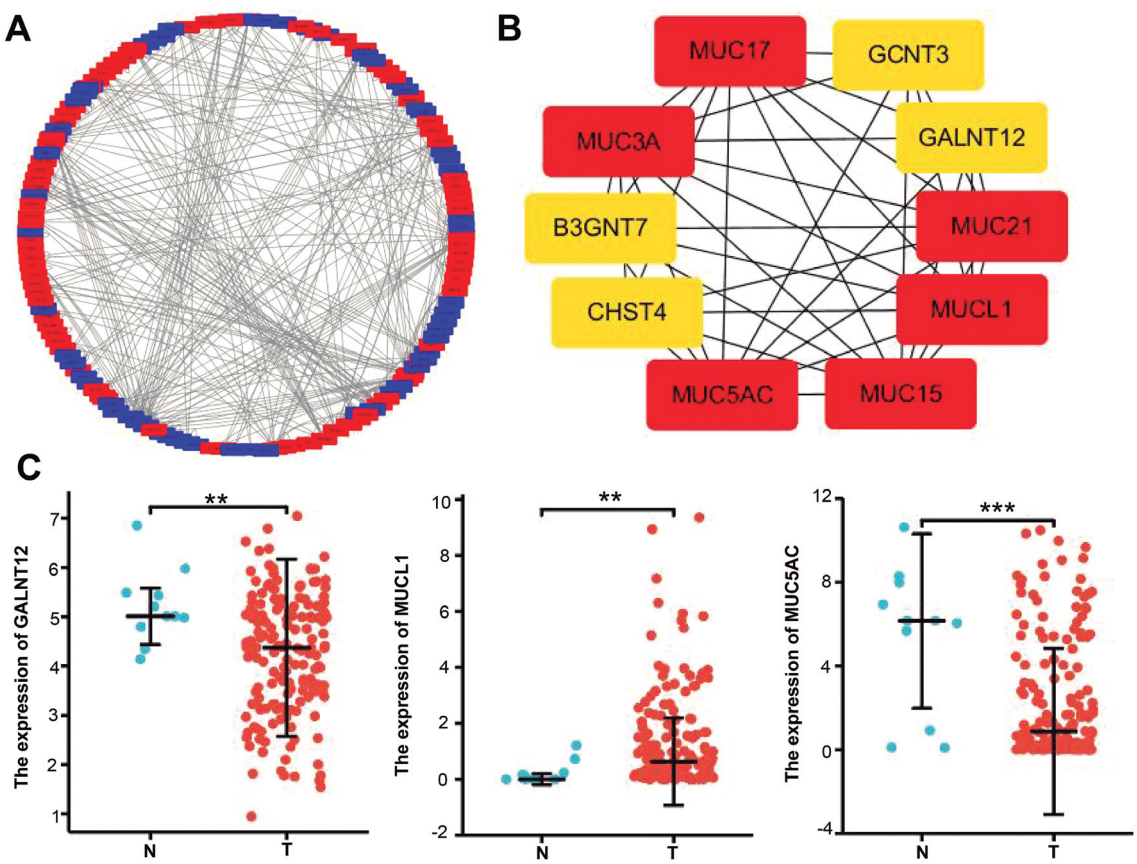

Fig. 3. The hub genes for Grin2d in esophageal cancer. STRING and Cytoscape were employed to screen the Grin2d hub genes in esophageal cancer **(A)**. The hotspot hub genes were selected **(B)** and compared between esophageal cancer and normal tissue **(C)**. N, normal; T, tumor; **, p<0.01; ***, p<0.001.

expressed in esophageal squamous epithelial cells but strongly expressed in well-differentiated esophageal adenocarcinoma and metastatic cancer in the lymph nodes (Fig. 5B). The Grin2d positive staining rates were 41.2% (159/386), 66.3% (333/502), and 58.6% (75/128) for normal esophageal mucosa, primary carcinoma, and lymph node metastasis, respectively (Table 2). Based on the frequency and density of the staining, Grin2d protein levels were higher in esophageal cancer than in normal mucosa (Table 2, $p<0.05$) and positively correlated with distal metastasis (Table 3, $p<0.05$). Kaplan-Meier analysis showed that Grin2d expression was associated with an unfavorable overall survival for esophageal carcinoma patients (Figure 5C, $p<0.05$); however, it was not an independent factor (Table 4, $p>0.05$)

The effects of Grin2d expression on the malignant phenotype of esophageal cancer cells

We successfully overexpressed and silenced Grin2d in KYSE-150 cells by transfecting a Grin2d overexpression or silencing vector, respectively (Fig. 6A). Grin2d overexpression promoted cellular proliferation, migration, and invasion while blocking

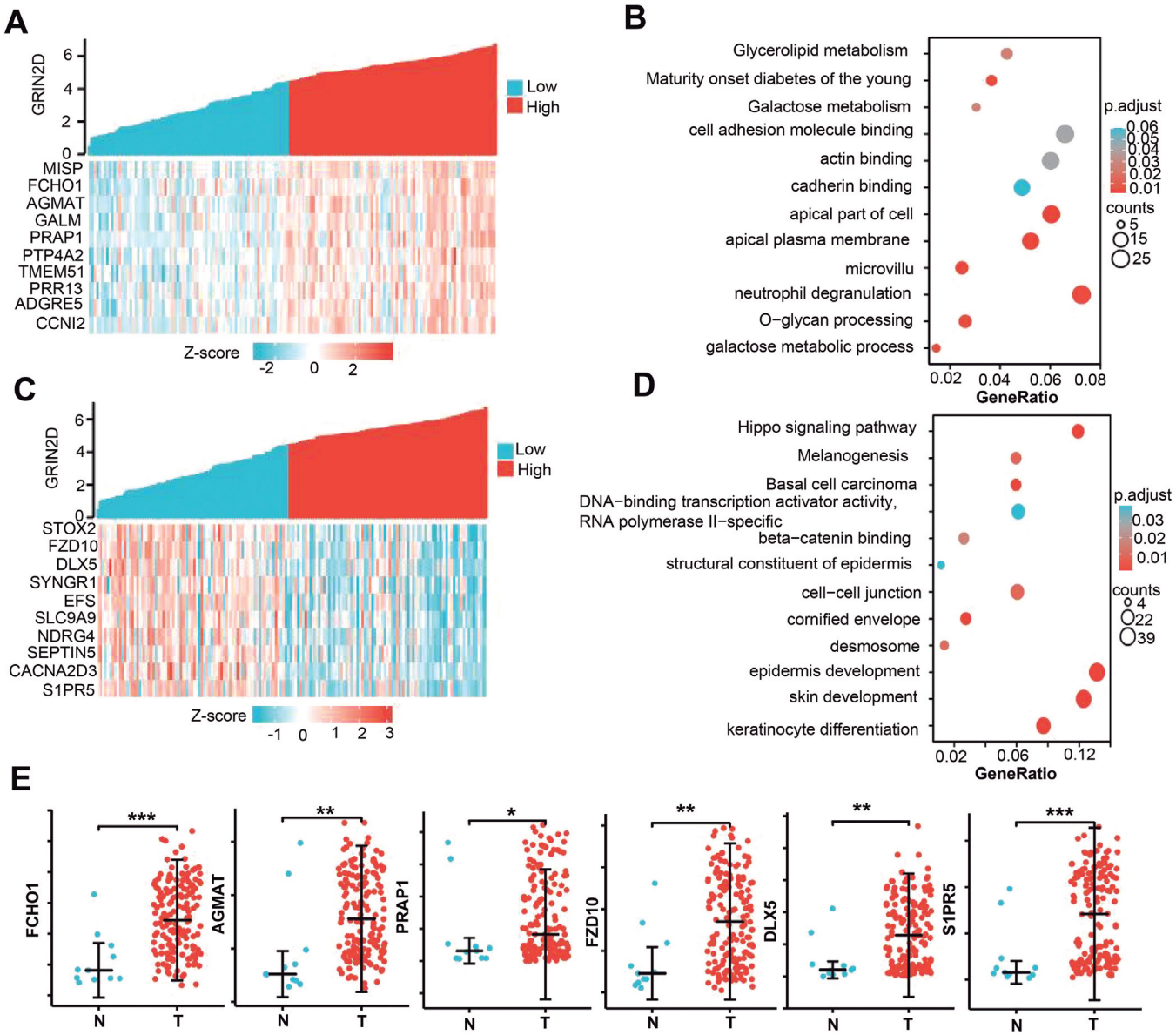

Fig. 4. The Grin2d-related genes and signaling pathways in esophageal cancer. The positively-related **(A, B)** and negatively-related **(C, D)** genes of Grin2d were screened and classified into signaling pathways using the xiantao database. The expression profiles and prognostic significance of these genes were also studied using the xiantao platform **(E)**. N, normal; T, tumor; *, $p<0.05$; **, $p<0.01$; ***, $p<0.001$.

apoptosis (Fig. 6B-E, p<0.05). Grin2d knockdown had the opposite effects on the KYSE-150 cells (Fig. 6B-E, p<0.05). Western blotting revealed that Grin2d overexpression increased Ki-67, PI3K, Akt, p-mTOR, p-CDC-25c, XIAP, Slug, and MMP-9 levels but decreased the expression of p27 and PARP-1 in these cells (Fig. 6F). Grin2d silencing had the opposite effects on this panel of genes (Fig. 6F).

Discussion

Grin2d expression is low and downregulated during the second week after birth. However, there is continuous Grin2d expression in the interneurons of

Table 4. Multivariate survival analysis of esophageal cancer patients.

Clinicopathological parameters	Relative risk (95%CI)	P
Age (≥65 years)	0.000 (0.000-6.420E+28)	0.750
Sex (female)	0.928 (0.579-1.488)	0.758
Depth of invasion (T3-4)	1.031 (0.673-1.578)	0.890
Venous invasion (+)	1.152 (0.696-1.906)	0.582
Lymph node metastasis (+)	0.191 (0.021-1.760)	0.144
Distant metastasis (+)	1.639 (0.682-3.939)	0.270
TNM staging (III-IV)	0.560 (0.249-1.263)	0.163
Differentiation (poorly differentiated)	0.089 (0.027-0.292)	<0.001
Tissue type(Adenocarcinoma)	0.374 (0.088-1.588)	0.182
Grin2d expression (+~+++)	0.746 (0.518-1.076)	0.117

CI, confidence interval.

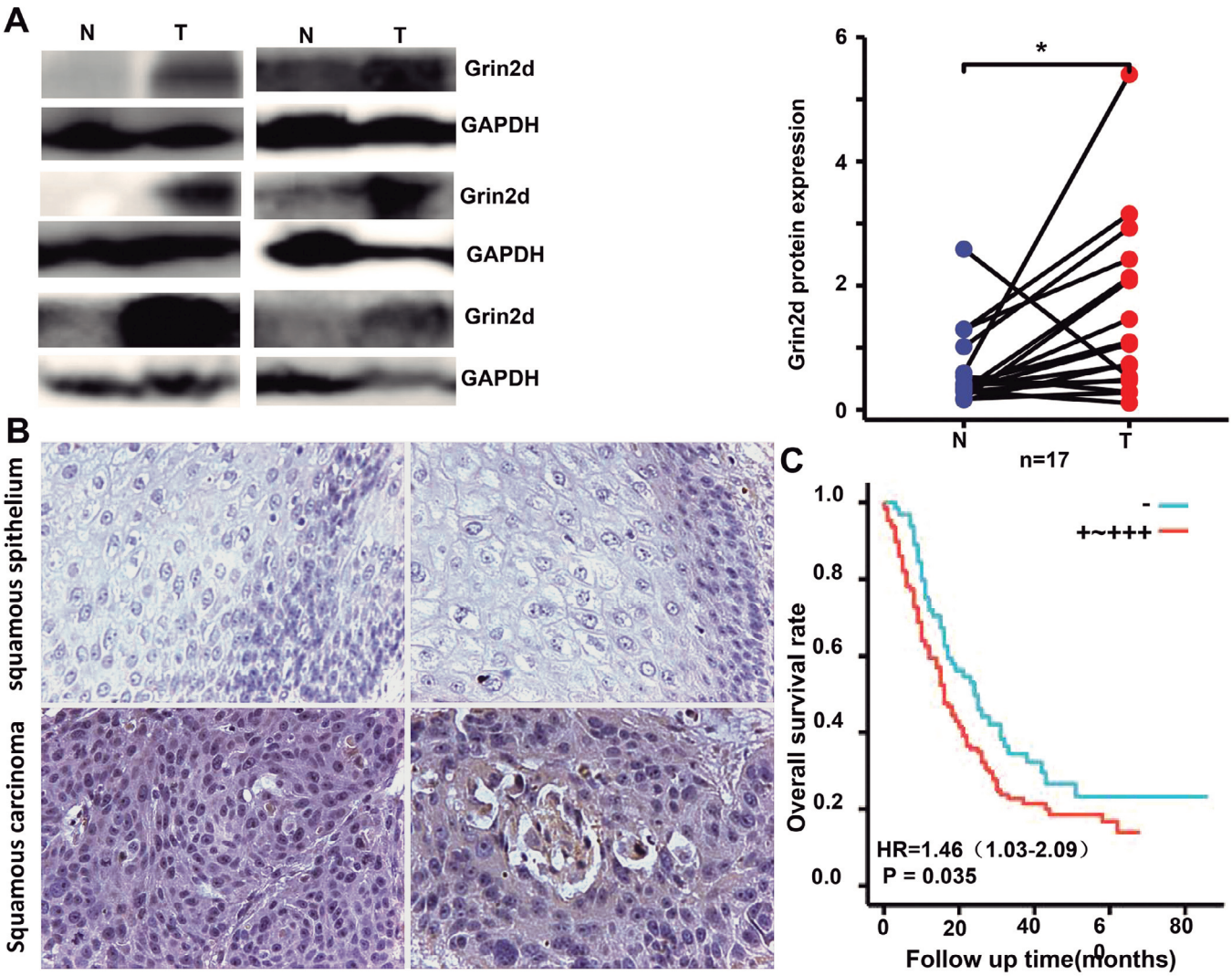

Fig. 5. The clinicopathological significances of Grin2d protein expression in esophageal cancer. Western blotting was used to determine Grin2d protein levels in esophageal cancer **(A)**. Densiometric analysis showed higher Grin2d protein levels in esophageal cancer than in normal tissue (**A**, p<0.05). Grin2d protein was also demonstrated in esophageal cancer by immunohistochemistry; it was only weakly detectable in normal squamous epithelial cells **(B)**. Kaplan-Meier curves and the log-rank test were used to clarify the prognostic significance of Grin2d protein expression **(C)**. N, normal; T, tumor; *, p<0.05.

juvenile mice. In transgenic Grin2d mice, GFP-tagged Grin2d was found in the hippocampal interneurons, most of which were also positive for parvalbumin or somatostatin. According to electrophysiological and morphological analysis, Grin2d mainly exists in the fast-spiking basket and axo-axonic cells. Moreover, Grin2d knockout mice showed that Grin2d-containing NMDARs could mediate synaptic currents in the hippocampal interneurons of young and juvenile mice and the CA1 pyramidal neurons of newborn mice (Von Engelhardt et al., 2015). These findings indicated that Grin2d might be involved in hippocampal memory.

Grin2d mRNA is steadily expressed in PC-3 and LNCAP human prostate cancer cells (Pissimissis et al., 2009), MG-63 human osteoblast-like osteosarcoma cells (Kalariti et al., 2004), giant cells (White et al., 2001), and human Y79 clonal retinoblastoma cells (Takeda et al., 2000). Brocke et al. (2010) found that Grin2d expression was higher in high- and low-grade astrocytomas compared to the normal human brain. Ferguson et al. (2016) found that Grin2d was specifically expressed in colorectal cancer vessels. Here, we observed Grin2d overexpression in esophageal cancer compared to normal mucosa. These data indicated that upregulated Grin2d expression levels might be involved in esophageal carcinogenesis.

Additionally, Grin2d mRNA expression levels were positively correlated with histological grading and the M stage of esophageal cancer. Grin2d protein levels were also positively related to remote metastasis and

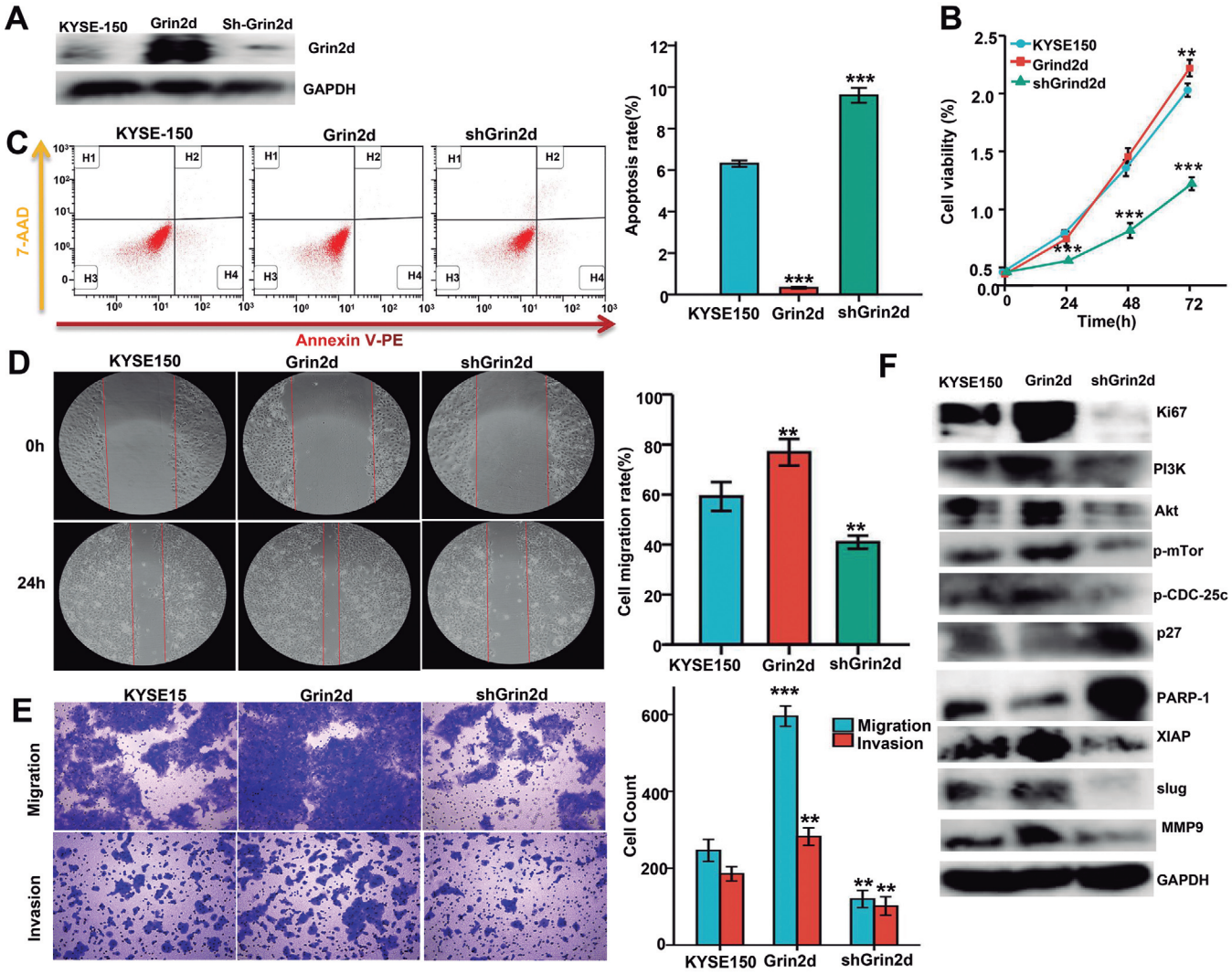

Fig. 6. The effects of Grin2d expression on esophageal cancer cells. Western blotting showed that Grin2d protein levels became stronger or weaker than the control after transfection of pcDNA3.1- Grin2d -3×Flag or pGPU6/GFP- shGrin2d into KYSE-150 cells, respectively **(A)**. The transfectants were subjected to functional assays for proliferation, apoptosis, migration, and invasion using the CCK-8 assay **(B)**, annexin V/7-AAD staining **(C)**, wound healing **(D)**, and transwell chambers **(E)**, respectively. The phenotype's proteins were screened by western blotting **(F)**. **, p<0.01; ***, p<0.001.

unfavorable prognosis in this disease. Grin2d expression is predictive of improved survival in colorectal cancer (Ferguson et al., 2016). These analyses demonstrated that Grin2d expression can indicate aggressive behavior and poor prognosis in esophageal cancer, although it was not an independent factor.

Yuan et al. (2016) found that downregulated miR-128 levels in low-grade glioma were closely related to glioma-associated epilepsy by targeting Grin2d. Li et al. (2020, 2022) found that miR-129-1-3p repressed the proliferation and migration of triple-negative breast cancer and prevented cardiomyocytes against pirarubicin-induced apoptosis by targeting Grin2d. Targeted knockdown and vaccination against the extracellular region of Grin2d reduced vascularization in the subcutaneous sponge angiogenesis assay. Immune-targeting of Grin2d in colorectal cancer has been demonstrated in mice; vaccination was able to inhibit colorectal tumor growth and vascularization (Ferguson et al., 2016). In the present study, Grin2d overexpression increased the proliferation, migration, and invasion and decreased apoptosis of esophageal cancer cells, whereas Grin2d knockdown had the opposite effects. These data indicated that Grin2d might promote the aggressive phenotype of esophageal cancer cells and be associated with the progression of esophageal cancer. According to our bioinformatics analysis, the Grin2d-related pathways included the metabolism of cholesterol, lipids, glycerolipids, galactose, and O-glycan, ABC transporters, cell adhesion binding, actin binding, cadherin binding, the Hippo signaling pathway, cell-cell junctions, desmosomes, and DNA-transcription activator binding, which might account for the influence of Grin2d on the aggressiveness of this disease.

Reportedly, p27 functions as a CDK inhibitor to arrest G1, and CDC-25c pushes cells into M phase (He et al., 2022). The PTEN/PI3K/Akt/mTOR pathway is one of the most frequently overactivated intracellular pathways involved in cell proliferation and the blocking of apoptosis in various cancers (Sanaei et al., 2022). XIAP can bind to and competitively suppress Caspase-3, 7, and 9, thereby inhibiting PARP1-mediated apoptosis (He et al., 2022). In esophageal cancer cells, Grin2d aggravated proliferation, disrupted the cell cycle, and weakened apoptosis by activating PTEN/PI3K/Akt/mTOR, up-regulating p-DC-25c and XIAP expression and suppressing p27 expression. Slug can promote migration, invasion, and the epithelial-mesenchymal transition (Fedele et al., 2022), and the MMPs are well known for breaking down the extracellular matrix and promoting metastasis (Wieczorek et al., 2015). Therefore, Grin2d might promote the migration and invasion of esophageal cancer cells by increasing Slug and MMP-9.

In summary, Grin2d appears to be involved in the pathogenesis and subsequent progression of esophageal cancer by enhancing proliferation, migration, and invasion and inhibiting apoptosis. Its aberrant expression might be employed as a biomarker to forecast the aggressive behaviors and unfavorable prognosis of esophageal cancer. It also might represent a novel therapeutic target.

Acknowledgements. Not applicable.

Funding. This study was supported by the Liaoning Distinguished Professor Award, Natural Science Foundation of Hebei Province (21377772D; H2022406034), the National Natural Scientific Foundation of China (81672700) and S&T Program of Chengde (202204A073).

Availability of data and materials. The datasets used and/or analyzed are available from the corresponding author on reasonable request.

Author contributions. Hua-chuan Zheng and Ling-ling Wang carried out the studies and wrote the main manuscript text. Jun Li, Hang Xue, Li Zhang, Da-yong Yu, Ning Yang, Wen-jing Yun, and Ming-zhen Zhao prepared figures and statistical analysis. All authors read and approved the final manuscript.

Ethics approval and consent to participate. Yes

Patient consent for publication. Yes

Competing interests. The authors declare that they have no competing interests.

References

Andrews W.T., Donahue D., Holmes A., Balsara R., Castellino F.J. and Hummon A.B. (2020). *In situ* metabolite and lipid analysis of GluN2D-/- and wild-type mice after ischemic stroke using MALDI MSI. Anal. Bioanal. Chem. 412, 6275-6285.

Brocke K.S., Staufner C., Luksch H., Geiger K.D., Stepulak A., Marzahn J., Schackert G., Temme A. and Ikonomidou C. (2010). Glutamate receptors in pediatric tumors of the central nervous system. Cancer Biol. Ther. 9, 455-468.

Camp C.R. and Yuan H. (2020). GRIN2D/GluN2D NMDA receptor: Unique features and its contribution to pediatric developmental and epileptic encephalopathy. Eur. J. Paediatr. Neurol. 24, 89-99.

Fedele M., Sgarra R., Battista S., Cerchia L. and Manfioletti G. (2022). The epithelial-mesenchymal transition at the crossroads between metabolism and tumor progression. Int. J. Mol. Sci. 23, 800.

Ferguson H.J., Wragg J.W., Ward S., Heath V.L., Ismail T. and Bicknell R. (2016). Glutamate dependent NMDA receptor 2D is a novel angiogenic tumour endothelial marker in colorectal cancer. Oncotarget 7, 20440-20454.

Hajdú T., Juhász T., Szűcs-Somogyi C., Rácz K. and Zákány R. (2018). NR1 and NR3B Composed Intranuclear N-methyl-d-aspartate Receptor Complexes in Human Melanoma Cells. Int. J. Mol. Sci. 19, 1929.

He S., Chakraborty R. and Ranganathan S. (2022). Proliferation and apoptosis pathways and factors in oral squamous cell carcinoma. Int. J. Mol. Sci. 23, 1562.

Kalariti N., Lembessis P. and Koutsilieris M. (2004). Characterization of the glutametergic system in MG-63 osteoblast-like osteosarcoma cells. Anticancer Res. 24, 3923-3929.

Li Q., Qin M., Tan Q., Li T., Gu Z., Huang P. and Ren L. (2020). MicroRNA-129-1-3p protects cardiomyocytes from pirarubicin-induced apoptosis by downregulating the GRIN2D-mediated Ca2+ signaling pathway. J. Cell Mol. Med. 24, 2260-2271.

Li Q, Gu Z, Tan Q, Ren L and Chen S (2022). MicroRNA-129-1-3p represses the progression of triple-negative breast cancer by targeting the *GRIN2D* gene. Biomed Res. Int. 2022, 1549357.

Ma J., Wang P., Huang L., Qiao J. and Li J. (2021). Bioinformatic analysis reveals an exosomal miRNA-mRNA network in colorectal cancer. BMC Med. Genomics 14, 60.

Musa I.H., Musa T.H., Musa H.H. and Ahmed M.E. (2021). Esophageal cancer epidemiology, diagnosis, and management in Sudan - A review. Med. J. Malaysia 76, 691-697.

Mwachiro M.M., Pritchett N., Calafat A.M., Parker R.K., Lando J.O., Murphy G., Chepkwony R., Burgert S.L., Abnet C.C., Topazian M.D., White R.E., Dawsey S.M. and Etemadi A. (2021). Indoor wood combustion, carcinogenic exposure and esophageal cancer in southwest Kenya. Environ. Int. 152, 106485.

Pałasz A. and Krzystanek M. (2022). Spider neurotoxins as modulators of NMDA receptor signaling. Neuromolecular Med. 24, 250-256.

Pissimissis N., Papageorgiou E., Lembessis P., Armakolas A. and Koutsilieris M. (2009). The glutamatergic system expression in human PC-3 and LNCaP prostate cancer cells. Anticancer Res. 29, 371-377.

Sanaei M.J., Razi S., Pourbagheri-Sigaroodi A. and Bashash D. (2022). The PI3K/Akt/mTOR pathway in lung cancer; oncogenic alterations, therapeutic opportunities, challenges, and a glance at the application of nanoparticles. Transl. Oncol. 18, 101364.

Takeda M., Haga M., Yamada H., Kinoshita M., Otsuka M., Tsuboi S. and Moriyama Y. (2000). Ionotropic glutamate receptors expressed in human retinoblastoma Y79 cells. Neurosci. Lett. 294, 97-100.

Von Engelhardt J., Bocklisch C., Tönges L., Herb A., Mishina M. and Monyer H. (2015). GluN2D- containing NMDA receptors-mediate synaptic currents in hippocampal interneurons and pyramidal cells in juvenile mice. Front. Cell. Neurosci. 9, 95.

White R., Hua Y., Scheithauer B., Lynch D.R., Henske E.P. and Crino P.B. (2001). Selective alterations in glutamate and GABA receptor subunit mRNA expression in dysplastic neurons and giant cells of cortical tubers. Ann. Neurol. 49, 67-78.

Wieczorek E., Jablonowski Z., Tomasik B., Konecki T., Jablonska E., Gromadzinska J., Fendler W., Sosnowski M., Wasowicz W. and Reszka E. (2015). MMP, VEGF and TIMP as prognostic factors in recurring bladder cancer. Clin. Biochem. 48, 1235-1240.

Wollmuth L.P., Chan K. and Groc L. (2021). The diverse and complex modes of action of anti-NMDA receptor autoantibodies. Neuropharmacology 194, 108624.

Yu M., Zheng H., Tsuneyama K., Takahashi H., Nomoto K., Xu H. and Takano Y. (2007). Paradoxical expression of maspin in gastric carcinomas: correlation with carcinogenesis and progression. Hum. Pathol. 38, 1248-1255.

Yuan Y., Xiang W., Yanhui L., Ruofei L., Yunhe M., Jiewen L. and Qing M. (2016). Dysregulation of microRNA-128 expression in WHO grades 2 glioma is associated with glioma- associated epilepsy: Downregulation of miR-128 induces glioma-associated seizure. Epilepsy Res. 127, 6-11.

Zarei Ghobadi M., Emamzadeh R., Teymoori-Rad M. and Mozhgani S.H. (2021). Decoding pathogenesis factors involved in the progression of ATLL or HAM/TSP after infection by HTLV-1 through a systems virology study. Virol. J. 18, 175.

Zhao H., Mei K., Yang L., Liu X. and Xie L. (2021). Green tea consumption and risk for esophageal cancer: A systematic review and dose-response meta-analysis. Nutrition 87-88, 111197.

Accepted November 9, 2023